Organic-Based ("Excitonic") Solar Cells

Brian A. Gregg
National Renewable Energy Laboratory
1617 Cole Blvd., Golden, CO 80401-3393

ABSTRACT

The existing types of organic-based solar cells, including dye-sensitized solar cells (DSSCs), can be categorized by their photoconversion mechanism as excitonic solar cells, XSCs. Their distinguishing characteristic is that charge generation and separation are simultaneous and this occurs via exciton dissociation at a heterointerface. Electrons are photogenerated on one side of the interface and holes on the other. This results in fundamental differences between XSCs and conventional PV cells. For example, the open circuit photovoltage, V_{oc}, in conventional cells is limited to less than the magnitude of the band bending, $Ø_{bi}$; however, V_{oc} in XSCs is commonly greater than $Ø_{bi}$. A general theoretical description is employed to quantify the differences between conventional and excitonic cells. The key difference is the dominant importance, in XSCs, of the photoinduced chemical potential energy gradient, $\nabla\mu_{h\nu}$, whereas $\nabla\mu_{h\nu}$ is unimportant, and therefore neglected, in theoretical descriptions of conventional PV cells. Several examples are provided.

1. Introduction

There is a well-known difference between the photoconversion mechanisms in inorganic photovoltaic (IPV) cells and in organic (excitonic) solar cells, XSCs: light absorption in XSCs leads to the production of excitons (mobile excited states), while in IPV cells it leads directly to the creation of free electron-hole pairs. This difference, has fundamental, and under-appreciated, consequences for the theoretical description of the photoconversion process, and also for efforts to optimize the performance of XSCs.

Light absorption in organic materials almost always results in the production of a mobile excited state rather than a free electron-hole pair because: 1) The dielectric constant of the organic phase is usually low compared to inorganic semiconductors, so the attractive Coulomb potential well around the incipient electron-hole pair extends over a greater volume than it does in inorganic semiconductors, and 2) The non-covalent electronic interactions between organic molecules are weak (resulting in a narrow band width) compared to the strong interatomic electronic interactions of covalently bonded inorganic semiconductor materials like silicon. Therefore, the electron's wavefunction is spatially restricted (small Bohr radius), allowing it to be localized in the potential well of its conjugate hole (and vice versa). This results in a tightly bound electron-hole pair (Frenkel exciton or mobile excited state) as the usual product of light absorption in organic semiconductors. It is a mobile, electrically neutral species which, to first order, is unaffected by electric fields.

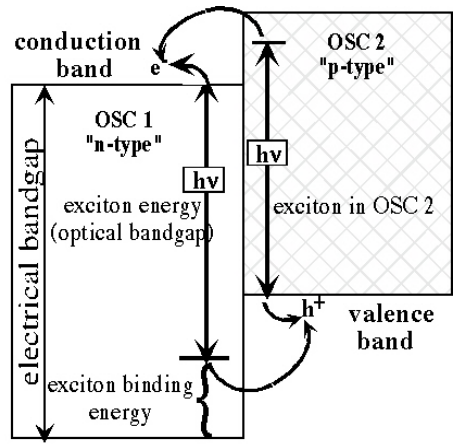

Figure 1. Energy level diagram for an XSC.

Excitons dissociate primarily at heterointerfaces resulting in electrons in one phase and holes, already separated from the electrons, in the other phase (Figure 1). Band bending, $Ø_{bi}$, although it can be useful, is not required to separate the charge carriers. The interfacial exciton dissociation process leads to large concentration gradients of the two carrier types at the interface.

2. Studies of Dye-Sensitized Solar Cells

The most advanced of the current XSCs, the DSSC, is a more complex structure than that shown in Fig. 1. Only one side (OSC2) is photoactive and it consists of just one monolayer of sensitizing dye, while OSC1 consists of a film of nanoporous TiO_2 with such a high surface area that the adsorbed monolayer of dye is optically thick. To make intimate electrical contact to such a convoluted film usually requires a liquid electrolyte solution. In order to minimize the rate of the recombination reaction, the kinetically ultra-slow redox couple iodine/tri-iodide is commonly employed.

Despite its structural complexity, the DSSC offers a particularly simple system in which to study the conceptual properties of XSCs because, in it, both exciton transport and internal electric fields are negligible. The former occurs because the organic layer is only one monolayer thick, the latter because the concentrated redox electrolyte solution permeating the entire TiO_2 film screens all electric fields within < 1 nm. DSSCs are thus essentially electric-field-free both at equilibrium and under illumination. However, we must carefully define what is meant by "field-free". In general, if there is no electric field in a solar cell at equilibrium, there must be a photogenerated electric field under illumination that opposes further charge separation. Such fields do exist in an illuminated DSSC, but the

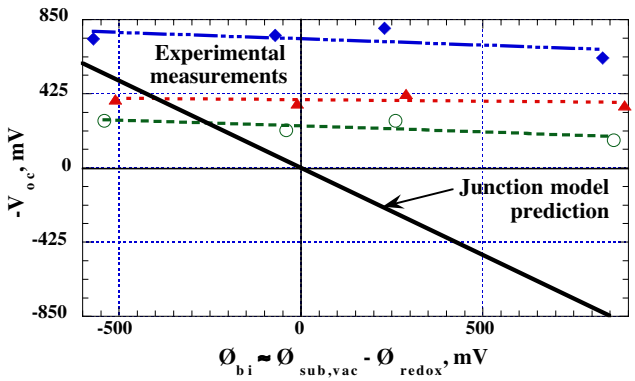

Figure 2. The open circuit photovoltage plotted *vs* the difference between the work functions of four different substrates in vacuum, $Ø_{sub,\ vac}$, and redox potentials, $Ø_{redox}$ of three different solutions. The work function of the substrate in the solution, $Ø_{sub}$, is difficult to measure directly but is related to $Ø_{sub,\ vac}$. The theoretical line (solid) shows the behavior predicted by the junction model.

concentrated electrolyte solution confines these photogenerated fields to such a small volume at the solid/solution interface that they present an insignificant barrier to carrier transport.

This understanding of DSSCs (and XSCs in general) is not universally accepted. Several groups postulated that the PV effect in DSSCs was driven by $Ø_{bi}$, as it is in conventional solar cells. The best-defined of these models predicts that the electrical potential difference (junction potential) between the F-SnO_2 substrate and the redox solution, falling across the first contacting particle of the TiO_2 film, sets an upper limit to the photovoltage in DSSCs. Therefore, DSSCs are subject to the same limitation as conventional solar cells: $qV_{oc} < Ø_{bi}$. We refer to this model as the "junction model". Given our experience with other XSCs, we were skeptical of this model since it neglected the force generated by asymmetric interfacial exciton dissociation. Building on the work of many others, we proposed the "interface model" that emphasized this interfacial force. To distinguish between the junction and interface models, we tested the dependence of V_{oc} on the difference ($\approx Ø_{bi}$) between the work functions of the substrate electrode and the redox solution. The junction model predicted a linear dependence, while we predicted little or no dependence of qV_{oc} on $Ø_{bi}$. The experimental results were unambiguous: V_{oc} was practically independent of $Ø_{bi}$ for four different substrates in three different redox solutions (Fig. 2).

This showed (again) that $Ø_{bi}$ does not determine V_{oc} in XSCs. Obviously, to understand XSCs we cannot rely on the models of conventional solar cells which are based on a number of assumptions that are not applicable to XSCs. To understand XSCs, we must at first avoid all of the usual assumptions, and start anew from the basic physics of solar cells.

3. $\nabla\mu_{h\nu}$ and the Photovoltage-Determining Mechanism

Conventional solar cells, almost by definition, function according to a mechanism epitomized by silicon p–n junction solar cells. This mechanism is so well known that the assumptions underlying it are sometimes forgotten and it is thought to be the only possible mechanism for photoconversion. It has often been applied incorrectly to describe XSC cells. Here, in the spirit of non-equilibrium thermodynamics, we review the generalized forces that drive a flux of electrons through a solar cell. This treatment does not make any device-specific assumptions, therefore it is valid for all types of solar cells.

The general kinetic expresssion for the one dimensional current density of electrons, $J_n(x)$, through any device is usually expressed as:

$$J_n(x)= n(x)\ \mu_n\ \nabla U\ (x) + k\ T\ \mu_n\ \nabla n(x) \qquad (1)$$

where $n(x)$ is the concentration of electrons, μ_n is the electron mobility (not to be confused with the chemical potential energy, μ) and k and T are Boltzmann's constant and the absolute temperature, respectively. An exactly analogous equation describes the flux of holes.

The quasi (i.e., non-equilibrium) Fermi level for electrons in a semiconductor is defined as:

$$E_{Fn}(x) = E_{cb}(x) + k\ T\ ln\{n(x)/N_c\} \qquad (2)$$

where $E_{cb}(x)$ is the electrical potential energy of the conduction band edge, $E_{cb}(x) = U(x)$ + constant; and N_c is the density of electronic states at the bottom of the conduction band. Taking the gradient of eq. 2 and substituting it into eq. 1 provides the simplest expression for the electron current:

$$J_n(x) = n(x)\ \mu_n\ \nabla E_{Fn}\ (x) \qquad (3)$$

Thus, whenever $\nabla E_{Fn} \neq 0$ ($\nabla E_{Fp} \neq 0$), an electron (hole) current will flow through the device.

Equation 3 shows that the flux of electrons (J_n) is related to the (photo)electrochemical force (∇E_{Fn}) by a proportionality factor ($n\ \mu_n$). Equation 3 and the related equation for holes can be employed as a simple and powerful description of solar photoconversion systems. For example, *any* photoprocess that generates a non-zero value of ∇E_{Fn} and/or ∇E_{Fp} will result in a photovoltaic effect. This can be accomplished in a number of different ways, only one of which is employed in conventional p–n junctions. It is useful to break ∇E_{Fn} into its component quasi-thermodynamic constituents, ∇U and $\nabla\mu$, to clearly reveal the difference between the photoconversion mechanisms of IPV and OPV cells. Eq. 1 can be separated into two independent electron fluxes, each driven by one of the two non-equilibrium forces, ∇U and $\nabla\mu$.

J_n due to the electrical potential energy gradient is:

$$J_n(x)= n(x)\ \mu_n\ \text{x}\ \nabla U(x) \qquad (4a)$$

J_n due to the chemical potential energy gradient is:

$$J_n(x)= n(x)\ \mu_n\ \text{x}\ k\ T/n(x)\ \nabla n(x)$$

or:

$$J_n(x)= n(x)\ \mu_n\ \text{x}\ \nabla\mu(x) \qquad (4b)$$

These equations are equally valid in the light and in the dark. We employ $\nabla\mu_{h\nu}$ and $\nabla U_{h\nu}$ to denote these forces in a cell under illumination.

Equation 3 can be rewritten as,

$$J_n(x)= n(x)\ \mu_n\ \{\nabla U(x) + \nabla\mu(x)\} \qquad (5)$$

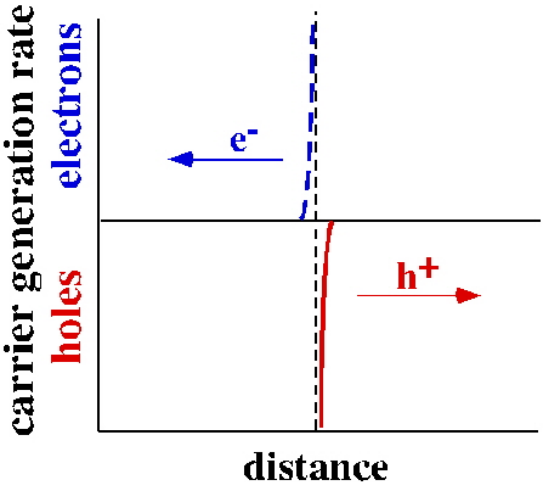

Figure 3. A schematic showing the characteristic carrier generation rates in XSCs. The heterointerface is represented by the dashed vertical line. The arrows represent the force, $\nabla\mu_{h\nu}$, on the photogenerated carriers. Recombination is also driven by $\nabla\mu_{h\nu}$, but this interfacial process is slow in any viable XSC.

Equation 5 shows that the electrical potential energy gradient, ∇U, and the chemical potential energy gradient, $\nabla\mu$, are *equivalent* forces. This equivalence is sometimes overlooked because of the predominant importance of ∇U in conventional PV cells. This results primarily from two factors: (1) the photogeneration of carriers throughout the bulk and, (2) the high carrier mobilities that allow them to quickly "equilibrate" their spatial distributions regardless of their point of origin. Both of these factors minimize the influence of $\nabla\mu_{h\nu}$ in conventional PV cells. However, in XSCs, almost all carriers are photogenerated in a narrow region near the interface, leading to a photoinduced carrier concentration gradient (proportional to $\nabla\mu_{h\nu}$) that is much higher and qualitatively distinct from that in conventional PV cells (Figure 3). This effect, coupled with the spatial separation of the two carrier types across the interface upon photogeneration, constitute a powerful photovoltaic driving force. This is further enhanced by the generally low equilibrium charge carrier density, making $\nabla\mu_{h\nu}$ often the dominant driving force in XSCs. For example, ∇U can be ~0 in the bulk and a highly efficient solar cell can be made based wholly on $\nabla\mu_{h\nu}$. This is how DSSCs function. In solid state organic PV cells without mobile electrolyte, both ∇U and $\nabla\mu$ must be taken into account.

The open circuit photovoltage, V_{oc}, occurs, of course, when the photodriven forward current is equal and opposite to the sum of the recombination currents. In general, the photovoltage of a solar cell is a function of *both* the built-in electrical *and* the photo-generated chemical potential energy differences across the cell (eq. 5). The common assumption that $\varnothing_{bi}$ (= $\int\nabla U\ dx$ at equilibrium) alone sets the upper limit to the photovoltage is clearly not true in general. However, it *is* approximately true for a specific photoconversion mechanism—that which governs conventional solar cells: When both electrons and holes are photogenerated together in the same semiconductor phase, and thus have the same spatial distribution, $\nabla\mu_{h\nu}(x)$ drives them both in the same direction (although it may be a small force, especially for majority carriers). To separate electrons from holes then requires the only other available force, $\nabla U_{h\nu}$. Therefore, in this case, $\varnothing_{bi}$ sets the upper limit to qV_{oc} *because* $\varnothing_{bi}$ is required for charge separation. (We ignore small effects such as Dember potentials for simplicity.)

Excitonic solar cells are fundamentally different. The charge carrier pairs are already separated across an interface upon photogeneration, creating a large $\nabla\mu_{h\nu}$ (Figure 3) which tends to separate them further. An internal electric field is not required for charge separation, and thus $\varnothing_{bi}$ does *not* set the upper limit to V_{oc}. Substantial PV effects can be achieved in both solid state XSCs and in DSSCs under conditions where $\varnothing_{bi} \approx 0$. Numerical simulations of DSSCs also have shown that V_{oc} can be nearly independent of $\varnothing_{bi}$, while simulations of organic PV cells showed that V_{oc} is commonly greater than $\varnothing_{bi}$.

The maximum photovoltage obtainable in any solar cell at a given light intensity, I, can be derived from eq. 5. Since ∇E_{Fn} and ∇E_{Fp} are the driving forces for the fluxes of electrons and holes, respectively, net current flow must stop when these gradients either simultaneously become zero (the ideal cell), or when the electron flux exactly cancels the hole flux (non-ideal cell). The maximum possible photovoltage in any PV cell is thus given by the maximum splitting between the quasi Fermi levels anywhere in the cell at open circuit, since an applied potential difference greater than this will cause the photocurrent to reverse its direction.

4. Numerical Simulations of Conventional PV Cells and XSCs

There are numerous differences between conventional semiconductors such as silicon and organic semiconductors such as perylene diimides or conducting polymers. To name just a few: there are major differences in bandwidths, Madelung constants, carrier mobilities, defect densities, dielectric constants, purities, doping levels, etc. All of these factors play an important role in the *quantitative* differences between conventional and excitonic solar cells. Yet, it is the theme of this paper that there is one unique factor that accounts for the *qualitative* differences between them: the spatial distribution of the photogenerated charge carriers (see Fig. 3). In order to demonstrate the significance of this seemingly small difference, we performed numerical simulations to compare two heterojunction solar cells (one "conventional" and one "XSC") in which every parameter was identical except the location of the photogenerated charge carriers.

The simulated cells incorporate band bending ($\varnothing_{bi}$ = 0.64 V) resulting from the assumed doping densities of $n_d = n_a = 10^{12}$ cm^{-3} on the left and right hand sides, respectively of the device, and ohmic contacts to each side (Fig. 4a). The bandgaps, band offsets and doping densities are loosely based on a perylene diimide/metallo-phthalocyanine cell (left and right hand sides, respectively).

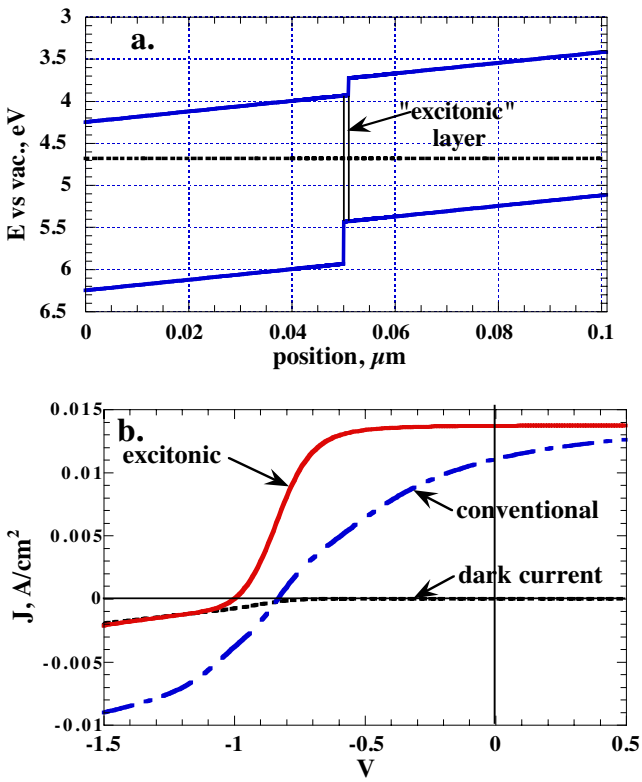

Figure 4. (a) Band diagram of the simulated solar cells (conventional and excitonic) at equilibrium. In the conventional cell, the exponential absorption coefficient is $\alpha = 10^5$ cm^{-1} throughout the cell; in the excitonic cell, light is absorbed only within 1 nm of the interface (the "excitonic layer") with $\alpha = 10^7$ cm^{-1}. (b) The calculated *J-V* curves under 50 mW/cm^2 illumination (31.6 mW/cm^2 is absorbed) at $\lambda = 2.1$ eV. The only difference between the conventional and excitonic cells is the spatial distribution of the photogenerated charge carriers. The dark current is identical for both devices.

We employed the simulation program SimWindow s, http://www.ocs.colorado.edu/SimWindows/simwin.html. It numerically solves the coupled differential equations (transport, continuity and Poisson's) that describe optoelectronic phenomena in semiconductor devices. By design, it equates light absorption with charge carrier generation. In order to adapt it to compare conventional to excitonic PV cells, we made the following assumption for the XSCs: light absorption occurs only in a 1 nm thick "excitonic layer" at the heterojunction between the two organic semiconductors. In other words, we neglect exciton transport and assume that all excitons are created and dissociate in the excitonic layer. We set the conduction band edge of the "excitonic layer" at the potential of the more positive semiconductor and the valence band edge at the potential of the more negative semiconductor. Light absorption in this layer thus naturally leads to electron transfer to the left, and hole transfer to the right as well as to recombination in the excitonic layer. This is a reasonable, but not perfect, approximation to the effect of the interfacial dissociation of excitons.

The excitonic layer was also included in the conventional PV device, but in this case, the light absorption coefficient was set constant throughout the cell. When illuminated, the light is incident on the left hand side. All carrier mobilities are set to 0.1 cm^2/V s. The only difference between the conventional and excitonic PV cells in our comparison is that the absorption coefficient is $\alpha = 10^5$ cm^{-1} everywhere throughout the 101 nm thick conventional PV cell, while $\alpha = 10^7$ cm^{-1} in the 1 nm thick "excitonic layer" of the XSC and $\alpha = 0$ cm^{-1} elsewhere. The amount of light absorbed is thus practically the same in both cells; only its spatial distribution, and therefore the spatial distribution of photogenerated charge carriers, differ between the simulated cells.

The simulation (Fig. 4b) shows that major differences in PV behavior occur in otherwise identical devices that differ *only* in the spatial distribution of photogenerated carriers. The conventional cell is much less efficient than the XSC. There are at least two reasons for this: (1) recombination throughout the bulk is more efficient than recombination only at the interface (excitonic layer), given the same rate constants for recombination. (2) As depicted in Fig. 3, the XSC has the photogenerated force, $\nabla\mu_{h\nu}$, operating in concert with $\varnothing_{bi}$ separating the two carriers and driving them toward their respective electrodes; while in the conventional cell, $\nabla\mu_{h\nu}$ opposes $\varnothing_{bi}$. Thus, the conventional cell produces $V_{oc} = 0.83$ V while the XSC produces $V_{oc} = 1.00$ V. (Both of these are greater than $\varnothing_{bi} = 0.64$ eV because the band offset at the heterojunction also serves to rectify the photocurrent.) The relative short circuit photocurrents (11.1 mA/cm^2 versus 13.7 mA/cm^2) and fill factors (34% vs 59%) strongly favor the XSC. Overall, the simulated XSC has a conversion efficiency more than 2.5 fold higher than the conventional cell. Having two driving forces working in concert (XSCs) is naturally better than having the two forces oppose one another (conventional cells), all else being equal. This is not meant to suggest that XSCs are inherently more efficient than conventional solar cells; most of the quantitative differences mentioned earlier still favor conventional cells. Nevertheless, it is clear that there are essential qualitative differences between the two general classes of solar cells. And, given further understanding and development, XSCs might eventually displace conventional solar cells by virtue of being cheaper and having comparable efficiencies.

For a more thorough discussion of these issues including a number of the relevant references, see:

Gregg, B. A. and Hanna, M. C. "Comparing organic to inorganic photovoltaic cells: Theory, experiment, and simulation", *J. Appl. Phys.* in press 15 March, 2003.

Gregg, B. A. "Excitonic Solar Cells", *J. Phys. Chem. B.* invited Feature Article, in press, spring-summer, 2003.